

Manganese-derived partial density of states in $\text{Cd}_{1-x}\text{Mn}_x\text{Te}$

L. Ley, M. Taniguchi,* J. Ghijsen, and R. L. Johnson

Max-Planck-Institut für Festkörperforschung, Heisenbergstrasse 1, D-7000 Stuttgart 80, Federal Republic of Germany

A. Fujimori

National Institute for Research in Inorganic Materials, Sakura-mura, Niihari-gun, Ibaraki 305, Japan

(Received 28 May 1986)

We have studied the contribution of Mn $3d$ states to the valence bands of $\text{Cd}_{0.35}\text{Mn}_{0.65}\text{Te}$ by means of the resonant enhancement of the Mn $3d$ photoionization cross section near the Mn $3p^53d^6(^6P)$ core excitation ($\hbar\omega=50$ eV). The cross section of selected valence-band areas has a characteristic resonance shape as a function of photon energy that is well described by a Fano-type profile. From the strength of the resonance we conclude that there is appreciable hybridization with Mn $3d$ states throughout the valence bands. In addition, a new interpretation of the photoemission intensity with strong Mn $3d$ character that lies in the ionic gap of the CdTe valence bands is given. Based on an analysis of the final-state structure in terms of a configuration-interaction calculation performed on a MnTe_4^{6-} cluster, we ascribe these features between 5 and 9 eV binding energy to d^4 final states (satellites), whereas the photoemission between 0 and 5 eV is due to Mn $3d$ multiplets where the d^4 final state is screened by charge transfer from the Te-derived valence-band states.

I. INTRODUCTION

$\text{Cd}_{1-x}\text{Mn}_x\text{Te}$ belongs to a class of semiconductors called semimagnetic because the replacement of the cation with magnetic Mn [configuration $3p^63d^5(^6S)$] leads to a number of novel magneto-optical and magnetotransport phenomena.¹⁻⁵ These effects derive from a hybridization of the localized Mn $3d$ states in the high-spin 6S configuration with the s - p band states of the crystal. In a recent photoemission study⁶ we investigated the contribution of the Mn $3d$ states to the valence-band (VB) density of states (DOS) in a series of $\text{Cd}_{1-x}\text{Mn}_x\text{Te}$ alloys ($0 \leq x \leq 0.65$) and came to the following conclusion concerning the hybridization of the Mn $3d^5(^6S)$ majority-spin manifold with the remainder of the band structure: The symmetry-adapted combinations of the $3d$ states of a Mn atom in a tetrahedral environment are E and T_2 , respectively. The E states do not hybridize strongly with the $5p$ states on the nearest-neighbor Te atoms on symmetry grounds and give rise to a sharp peak 3.4 eV below the valence-band maximum (VBM). A similar feature at comparable energies has been observed in $\text{Hg}_{1-x}\text{Mn}_x\text{Se}$ and $\text{Cd}_{1-x}\text{Mn}_x\text{Se}$.^{7,8} Utilizing the energy dependence of the partial photoionization cross sections of the atomic orbitals, we further deduced a nearly homogeneous contribution of the remaining three states of T_2 symmetry to the top 5 eV of the VB DOS. Features between 5 and 8 eV, i.e., below the bottom of the VB DOS in pure CdTe (excluding the Te $5s$ states at -10 eV) were also tentatively assigned to states with mixed Mn $3d$ -Te $5p$ character.

It is the purpose of the present paper to investigate the degree of hybridization in $\text{Cd}_{0.35}\text{Mn}_{0.65}\text{Te}$ further using resonant photoemission. The photoemission intensity of Mn $3d$ -derived features in the VB DOS is resonantly enhanced for photon energies near the Mn $3p \rightarrow 3d$ core excitation of about 50 eV. The resonant enhancement is a

many-body effect in which the $3p^53d^6$ core excitation decays into the continuum state $3p^63d^4\epsilon f$ (autoionization). The process has been treated theoretically by Davis and Feldkamp⁹ and it occurs in atomic¹⁰ as well as metallic Mn.¹¹ The resonance has been observed for the Mn $3d$ states at 3.4 eV below the VBM in $\text{Cd}_{1-x}\text{Mn}_x\text{Se}$ by Francoisi *et al.*⁸

The spectral dependence of the photoemission cross section near the resonance is determined by the interference between the discrete autoionization transition and the continuum of the normal one-electron emission because both lead, starting from the $3p^63d^5$ ground state, to the same final state $3p^63d^4\epsilon f$. The line shape of the resonance, $I(\omega)$, follows the result first derived by Fano:¹²

$$I(\omega) = I_0(\omega) \frac{(q+E)^2}{1+E^2} + I_{NR}(\omega), \quad (1)$$

where $I_0(\omega)$ is the $3d$ emission in the absence of the autoionizing transition and $I_{NR}(\omega)$ is a noninterfering background contribution. The asymmetry parameter q is determined by the magnitude and sign of the transition and interaction matrix elements and $E = (\hbar\omega - E_0)/\Gamma$ is a reduced energy expressed in terms of the energy E_0 and the width Γ of the resonance. Since only Mn $3d$ states are resonantly enhanced by this process, we shall estimate their contribution to the VB DOS by comparing spectra taken on and off resonance. This has the advantage that the cross sections of the remaining valence states (Te $5p$; Cd $5p, 5s$) (Ref. 13) do not vary appreciably over the small energy range of the resonance.

II. RESULTS AND ANALYSIS

The experiments were performed on the Flipper-II beamline at the storage ring DORIS (Doppel-Ring Speicheranlage), Deutsches Elektronen-Synchrotron

DESY, Hamburg, Germany, under the same conditions described earlier.⁶ Figure 1 shows a series of valence-band spectra of $\text{Cd}_{0.35}\text{Mn}_{0.65}\text{Te}$ for photon energies between 45.0 and 54.0 eV. The intensities have been normalized to the monochromator output. We notice the prominent resonance of the Mn $3d(E)$ states, 3.4 eV below the VBM, that reaches its maximum at a photon energy of 49.9 eV. The remainder of the valence bands is also resonantly enhanced, albeit to a lesser extent. In particular, a set of states shows up clearly between 5 and 8 eV binding energy near resonance that is undetectable off resonance. These are the new Mn-derived states we referred to earlier.

The shape of the resonance and its magnitude is best studied in the form of constant-initial-state (CIS) spectra which trace the photoemission cross section as a function of photon energy. Such spectra are presented for selected regions of the valence bands (identified by their binding energy E_i relative to VBM) in the upper half of Fig. 2. The spectra are corrected for variations in photon flux and can be compared not only with respect to the shape of the resonance but also in terms of relative intensities.

The relationship between the valence-band resonances and the Mn $3p \rightarrow 3d$ core excitation is apparent by a comparison with the corresponding absorption spectra of $\text{Cd}_{0.35}\text{Mn}_{0.65}\text{Te}$ and atomic Mn which are shown in the lower half of Fig. 2. The spectrum of $\text{Cd}_{0.35}\text{Mn}_{0.65}\text{Te}$ was obtained in the form of a constant-final-state (CFS) spectrum and that of atomic Mn is from Ref. 14. Absorption

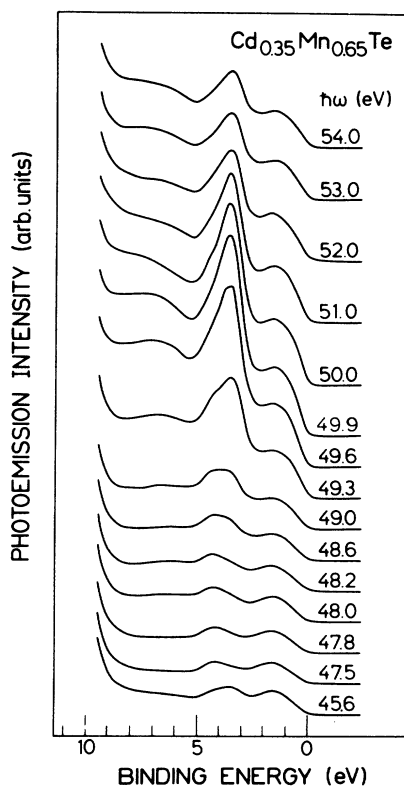


FIG. 1. A series of valence-band spectra of $\text{Cd}_{0.35}\text{Mn}_{0.65}\text{Te}$ for photon energies near the Mn $3p^3d^6(^6P)$ core excitation.

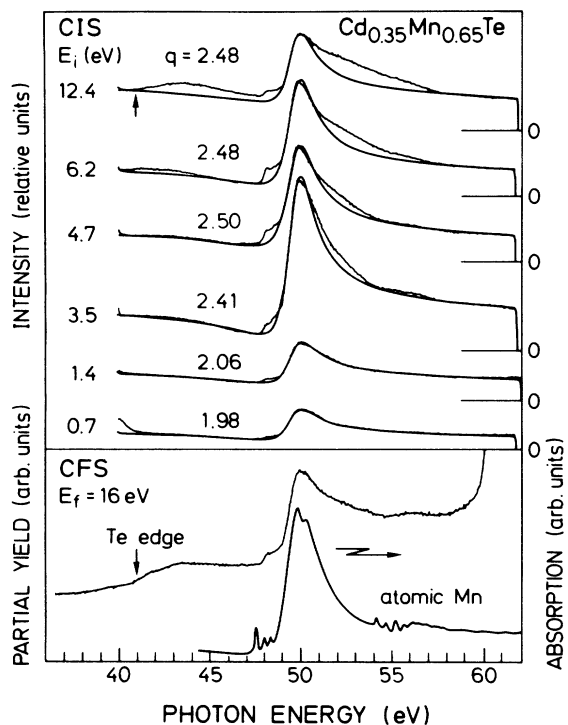


FIG. 2. (a) Constant-initial-state (CIS) spectra of selected valence-band regions that are identified by their initial state or binding energy E_i . The jagged line represents the data and the smooth line is a fit with a Fano profile; the relevant parameter q is given next to each spectrum. (b) Constant-final-state (CFS) spectrum of $\text{Cd}_{0.35}\text{Mn}_{0.65}\text{Te}$ and the Mn vapor absorption spectrum in the region of the Mn $3p \rightarrow 3d$ excitation.

between 47 and 50 eV in the latter is due to the Mn $3p \rightarrow 3d$ core transitions and the different structures are due to different multiplets of the final $3p^5 3d^6$ configuration. The strongest feature at 50 eV is the 6P multiplet, the only dipole-allowed transition from the 6S ground state in L - S coupling. This transition owes its width and asymmetry to the interference process that gives rise to the resonant enhancement of the Mn $3d$ photoemission cross section.⁹

The Mn $3p \rightarrow 3d$ absorption spectrum is seen to carry over with some solid-state broadening to $\text{Cd}_{0.35}\text{Mn}_{0.65}\text{Te}$. Small shifts in energy and a slight change in the shape of the 6P resonance have been discussed earlier.⁶ In addition, the Te $4d$ core absorption threshold is seen at 41.3 eV in the $\text{Cd}_{0.35}\text{Mn}_{0.65}\text{Te}$ spectrum.

For a further analysis of the CIS spectra we have fitted the principal 6P resonance to the line shape of Eq. (1). All fits were performed with the same $E_0 = 49.55 \pm 0.05$ eV and $\Gamma = 0.85$ eV allowing for an instrumental broadening of 0.15 eV. The asymmetry parameters q obtained from the fits are given next to each spectrum; they are generally around 2.45 and drop to about 2.0 for $E_i \leq 2.2$ eV. The q values agree in sign and magnitude quite well with that obtained for the 6P absorption resonance in atomic Mn, whereas the width of the resonance (Γ) as determined

from the CIS spectra of $\text{Cd}_{0.35}\text{Mn}_{0.65}\text{Te}$ is only about half of what it is in Mn .⁹

As intended, the fits do not cover the sharp resonances due to 6F and 6D final states that precede the main resonance. Taking that into consideration, the experimental CIS spectra are very well described by a single Fano profile for $E_i \leq 3.5$ eV. For higher E_i deviations occur in the energy region below 45 eV as well as on the high-energy side of the resonance. In particular, the low-energy part of the spectra for $E_i \geq 6.2$ eV becomes similar to the Te $4d \rightarrow \text{CB}$ transitions (where CB denotes conduction band) as seen in the CFS. A resonant enhancement of the Te $5p, 5s$ -derived VB states can be excluded because no resonance is observed for this photon energy range in the CIS spectra corresponding to the topmost parts of the VB ($E_i = 0.7$ and 1.4 eV) which have predominantly Te $5p$ character.¹³ Instead, we suggest that noncoherent, normal Auger decay channels contribute increasingly to the CIS spectra as we move away from the top of the valence bands and the shape of the CIS spectra approaches that of the optical absorption. It should be emphasized, however, that even for $E_i = 6.2$ eV the CIS spectrum is *mainly* determined by the direct recombination of the Mn $3p^5 3d^6 ({}^6P)$ resonance rather than by incoherent Auger decay as judged by the weak contributions from the Te $4d \rightarrow \text{CB}$ transitions around 44 eV and the other Mn $3p^5 3d^6$ multiplets above 51 eV, as well as by the pronounced asymmetry of the main resonance with a q value not different from the remainder of the spectra. In addition, we find that the Mn $M_{2,3}M_{4,5}M_{4,5}$ Auger emission is too weak to be observed even in spectra taken well above the resonance. This indicates that the predominant decay channel of the 6P excitation is by direct recombination (autoionization) rather than by Auger decay, consistent with the fairly localized nature of the 6P excitation.

We realize our aim to deduce a measure of the Mn $3d$ contribution to the VB DOS of $\text{Cd}_{0.35}\text{Mn}_{0.65}\text{Te}$ in the following way. According to Fig. 2 the Mn contribution is at its maximum on resonance at 49.9 eV and is at its minimum at a photon energy only 2 eV lower. We there-

fore subtract a spectrum recorded at the antiresonance ($\hbar\omega = 47.83$) from one taken at 49.9 eV, i.e., right on resonance after the intensities of both spectra have been normalized to the monochromator output. The result shown as curve *c* in Fig. 3 can be regarded as an estimate of the Mn $3d$ partial density of states. We find indeed appreciable Mn $3d$ contributions throughout the valence band. Since the Te $4d$ contribution disappears in the difference spectra, we realize that the new VB features extend down to about 9 eV binding energy. The Mn partial density of states is superimposed on a background of inelastically scattered electrons which extends below 9 eV. Since these electrons originate from primary emission with Mn $3d$ character, they are also resonantly enhanced and are thus responsible for the Fano resonance at $E_i = 12.4$ eV in Fig. 2.

III. DISCUSSION

Our earlier interpretation of the photoemission spectra of $\text{Cd}_{1-x}\text{Mn}_x\text{Te}$ was based on a one-electron description in terms of a valence-band density of states of mixed Mn $3d$ -Te $5p$ (Cd $5s, 5p$) character. This picture is in contrast to the case of MnO , for example, where the Mn $3d$ contribution to the photoemission spectrum is governed by the multiplet structure of the Mn $3d^4$ final state.¹⁵ Our argument was that the strong hybridization of the Mn $3d$ states with t_2 symmetry with the Te $5p$ states on neighboring atoms reduces the correlation energy sufficiently to allow a description in terms of band states. In the meantime, a number of band-structure calculations^{16,17} have been performed, none of which reproduce the additional states between 5 and 9 eV which are quite prominent according to our present analysis. This has led us to reconsider the interpretation of the Mn $3d$ -derived photoemission spectrum in $\text{Cd}_{1-x}\text{Mn}_x\text{Te}$.

To this end we have performed a configuration-interaction (CI) calculation on a model cluster, MnTe_4^{6-} , following the similar calculations for nickel compounds by Fujimori, Minami, and Sugano.¹⁸ The model represents a Mn^{2+} ion interacting with the filled Te $5p$ band; the Coulomb and exchange interaction of Mn $3d$ electrons are exactly treated while the Te $5p$ electrons are assumed to be uncorrelated. The ground-state covalency and the final-state charge transfer between Mn $3d$ and Te $5p$ (ligand) orbitals are treated on the same footing by considering CI between, e.g., d^n and $d^{n+1}\underline{L}$ configurations mediated by the d -ligand orbital hybridization. Then the ground state with ${}^6A_1 ({}^6S)$ symmetry is given by

$$\psi_g({}^6A_1) = a |d^5({}^6A_1)\rangle + b |d^6\underline{L}_\sigma({}^6A_1)\rangle + c |d^6\underline{L}_\pi({}^6A_1)\rangle, \quad (2)$$

and the final state with ${}^{2S+1}\Gamma$ symmetry by

$$\psi_f({}^{2S+1}\Gamma) = a' |d^4({}^{2S+1}\Gamma)\rangle + b' |d^5\underline{L}_\sigma({}^{2S+1}\Gamma)\rangle + c' |d^5\underline{L}_\pi({}^{2S+1}\Gamma)\rangle, \quad (3)$$

where \underline{L}_π and \underline{L}_σ denote E - and T_2 -symmetry ligand holes, respectively. The first term on the right-hand side of Eq. (2) [Eq. (3)] represents a purely ionic Mn^{2+} [Mn^{3+}] state and the second and third terms

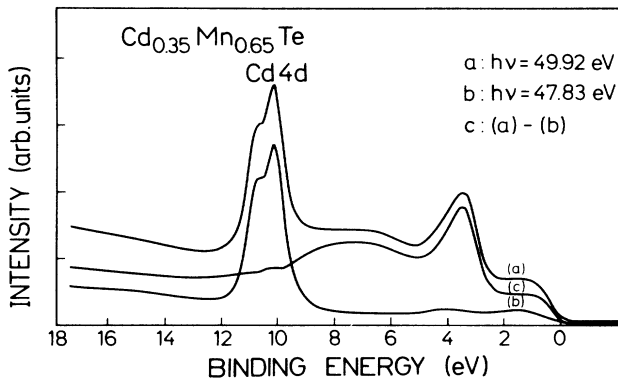


FIG. 3. Valence-band spectra of $\text{Cd}_{0.35}\text{Mn}_{0.65}\text{Te}$ taken at 49.9 (on resonance) and at 47.8 eV (antiresonance) photon energy. The difference spectrum is a measure of the Mn $3d$ partial density of states.

represent states where one electron is transferred from the ligand to d orbitals. The multiplet splitting (or equivalently the Racah parameters) of free Mn ions¹⁹ has been used, and energy differences between configurations, $E(d^5 \rightarrow d^5 \underline{L})$ and $E(d^4 \rightarrow d^5 \underline{L})$ (averaged over d^4 , d^5 , or d^6 multiplets), have been treated as adjustable parameters. The Mn $3d$ -Te $5p$ hybridization parameters ($pd\sigma$) and ($pd\pi$) were also allowed to vary with the constraint $(pd\sigma)/(pd\pi) = -2.17$ given by Harrison.²⁰ Details of the calculations will be presented elsewhere.²¹

The result is shown in Fig. 4, where one can see a reasonable agreement between theory and experiment.²² For the sake of comparison, the line spectrum has been convoluted with Gaussian (representing instrumental broadening and finite bandwidth effects) and Lorentzian (lifetime broadening which increases with increasing binding energies) functions. A background of inelastically scattered electrons has been added according to the description of Ref. 23. It should be noted that the peak at 3.4 eV is due mainly to a 5E final state produced by an electron emission, but there is also a 5T_2 final state in the same energy region. In addition, the 3.4-eV has predominantly $d^5 \underline{L}$ final-state character originating from $L \rightarrow d$ charge-transfer screening of d -hole (d^4) states. The satellite region (5–9 eV), on the contrary, is more d^4 -like without significant $L \rightarrow d$ screening. The satellite consists of 5E and 5T_2 states separated by 0.8 eV, while two peaks separated by ≥ 1 eV are discernible in the spectra of Ref.

6. Emission with Mn $3d$ character in the Te $5p$ VB region is due to one-electron Mn $3d$ -Te $5p$ hybridization and reflects the band density of states, as can be seen from the fact that the final-state configuration of this emission is almost purely $d^5 \underline{L}$, e and t_2 holes being screened by $L_\pi \rightarrow e$ and $L_\sigma \rightarrow t_2$ charge transfer, respectively, just as in a one-electron hybridization picture. We note that the hybridization in the 5T_2 final states is not necessarily much larger than that in the 5E final states as assumed by us earlier: the sharp 3.4-eV peak contains 5T_2 emission, and 5E -symmetry d -hole states are hybridized appreciably in the satellite and Te $5p$ valence-band regions.

The adjustable parameters are determined as $E(d^5 \rightarrow d^5 \underline{L}) = 3.5 \pm 1$ eV, $E(d^4 \rightarrow d^5 \underline{L}) = -4.0 \pm 0.3$ eV, $(pd\sigma) = -1.03 \pm 0.06$ eV, and $(pd\pi) = 0.47 \pm 0.03$ eV. These correspond to a Coulomb correlation energy $U \sim 8$ eV. The value for U is of the same order of magnitude as usually assumed for Mott insulators such as MnO, CoO, and NiO.^{18,24} The present U is for bare d electrons while U 's obtained by Fazzio *et al.*²⁵ include $L \rightarrow d$ charge-transfer effects and thus are much smaller. The number of Mn $3d$ electrons in the ground state is found to increase from that of the purely ionic value 5, to 5.1 ± 0.05 due to covalency, i.e., from Mn^{2+} to $Mn^{1.9+}$. Thus ~ 0.1 electron per Mn atom is transferred from the Te $5p$ VB to the empty Mn $3d$ minority-spin band, resulting in a net polarization of the valence electrons in the vicinity of the Mn atom and consequently in the interesting magneto-optical and magnetotransport properties. Also, superexchange interactions between Mn ions which lead to antiferromagnetic ordering are mediated by the same Mn $3d$ -VB hybridization.

IV. CONCLUSIONS

The new photoemission results and their analysis as presented here modify our earlier interpretation of the photoemission measurements of $Cd_{1-x}Mn_xTe$. The spectral density between 5 and 9 eV is not part of the valence-band density of states as assumed earlier but represents a satellite multiplet structure due to unscreened Mn $3d^4$ final states. We confirm, however, the Mn $3d$ -Te $5p$ hybridization which allows for sufficient screening of the $3d$ excitations by $L \rightarrow d$ charge transfer in the valence band. In that sense we consider the spectral density between 0 and 5 eV binding energy to a good approximation a measure of the valence density of states.

Our results are in contrast to the case of $Cd_{1-x}Mn_xSe$. Franciosi *et al.*⁸ conclude that in this system only the peak at 3.4 eV binding energy has Mn $3d$ character and that there is no evidence for d - p hybridization. In our model for the electronic structure of $Cd_{1-x}Mn_xTe$ the degree of Mn $3d$ -Te $5p$ hybridization depends—aside from the orbital overlap—on the energy difference between the two orbital energies after taking a 4-eV exchange splitting of the Mn $3d$ manifold into account. Using atomic term values this difference is ~ 4 eV for Mn $3d$ and Te $5p$ and ~ 3 eV for Mn $3d$ relative to Se $4p$. We would therefore expect appreciable hybridization also in $Cd_{1-x}Mn_xSe$.

The Mn $3p^3 3d^6 ({}^6P)$ excitation appears to decay mainly through autoionization, the process that leads to observed

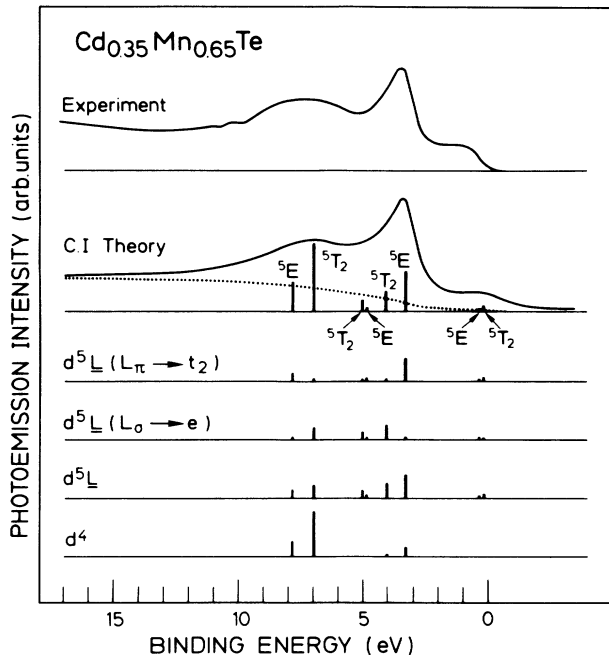


FIG. 4. The Mn $3d$ -derived part of the photoemission spectrum of $Cd_{0.35}Mn_{0.65}Te$ as derived in this figure is compared with the result of a CI calculation for a $MnTe_4^{6-}$ cluster. The multiplet lines have been lifetime and resolution broadened as described in the text. On the bottom final states are decomposed into the d^4 and $d^5 \underline{L}$ components.

valence band resonances. The normal Auger decay is weak by comparison.

ACKNOWLEDGMENTS

We are grateful to R. R. Galazka of the Institute of Physics, Warsaw, and to J. K. Furdyna of Purdue University for supplying the samples, to Professor Cardona for a

critical reading of the manuscript, and to H. Kölln for technical support. One of us (M.T.) would like to thank Professor M. Cardona for his hospitality and the Alexander von Humboldt Foundation (Bonn, Germany) for financial support. This project was partially financed by the Bundesminister für Forschung und Technologie (BMFT), Bonn, Germany.

*Present address: Synchrotron Radiation Laboratory, Institute for Solid State Physics, The University of Tokyo, Tanashi, Tokyo 188, Japan.

¹R. R. Galazka and J. Kossert, in *Narrow Gap Semiconductors: Physics and Applications*, Vol. 133, of *Lecture Notes in Physics* (Springer, Berlin, 1980).

²T. Dietl, *Solid State Sci.* **24**, 344 (1981).

³R. Reifenberger and D. A. Schwarzkopf, *Phys. Rev. Lett.* **50**, 907 (1983).

⁴J. K. Furdyna, *Proc. Int. Soc. Opt. Eng.* **409**, 43 (1983).

⁵A. E. Turner, R. L. Gemshov, and S. Datta, *Appl. Opt.* **22**, 3152 (1983).

⁶M. Taniguchi, L. Ley, R. L. Johnson, J. Ghijsen, and M. Cardona, *Phys. Rev. B* **33**, 1206 (1986).

⁷A. Franciosi, C. Caprile, and R. Reifenberger, *Phys. Rev. B* **31**, 8061 (1985).

⁸A. Franciosi, S. Chang, R. Reifenberger, U. Debska, and R. Riedel, *Phys. Rev. B* **32**, 6682 (1985).

⁹L. C. Davis and L. A. Feldkamp, *Phys. Rev. A* **17**, 2012 (1978); *Phys. Rev. B* **23**, 6239 (1981).

¹⁰J. P. Connerade, M. W. D. Mansfield, and M. A. P. Martin, *Proc. R. Soc. London, Sec. A* **350**, 405 (1976).

¹¹B. Sonntag, R. Haensel, and C. Kunz, *Solid State Commun.* **7**, 597 (1969).

¹²U. Fano, *Phys. Rev.* **124**, 1866 (1961).

¹³L. Ley, R. A. Pollak, F. R. McFeely, S. P. Kowalczyk, and D. A. Shirley, *Phys. Rev. B* **9**, 600 (1974).

¹⁴H. Köberle, Ph.D. thesis, University of Hamburg, 1985 (unpublished).

¹⁵D. E. Eastman and J. L. Freeouf, *Phys. Rev. Lett.* **34**, 395 (1975).

¹⁶B. Velický, J. Masek, and V. Chab, *Acta Phys. Pol., Ser. A* **69**, 1059 (1986).

¹⁷Z. Wei and A. Zunger, *Phys. Rev. Lett.* **56**, 2391 (1986).

¹⁸A. Fujimori, F. Minami, and S. Sugano, *Phys. Rev. B* **29**, 5225 (1984); A. Fujimori and F. Minami, *ibid.* **30**, 957 (1984).

¹⁹Y. Tanabe and S. Sugano, *J. Phys. Soc. Jpn.* **9**, 767 (1954).

²⁰W. A. Harrison, *Electron Structure and the Properties of Solids* (Freeman, San Francisco, 1980).

²¹A. Fujimori, M. Saeki, N. Kimizuka, M. Taniguchi, and S. Suga (unpublished).

²²The calculation of the photoemission intensities has been done by using matrix elements for direct photoemission $3d^n \rightarrow 3d^{n-1}el$, although the present experimental d -derived intensities are largely determined by matrix elements for super-Coster-Kronig transitions $3p^3 3d^{n+1} \rightarrow 3d^6 3d^{n-1}el$. However, neglecting the matrix-element difference between both cases may be justified by the similarity between the present d -derived spectrum and the difference spectrum.

²³D. A. Shirley, *Phys. Rev. B* **5**, 4709 (1972).

²⁴B. H. Brandow, *Adv. Phys.* **26**, 651 (1977).

²⁵A. Fazzio, M. J. Caldas, and A. Zunger, *Phys. Rev. B* **30**, 3430 (1984).